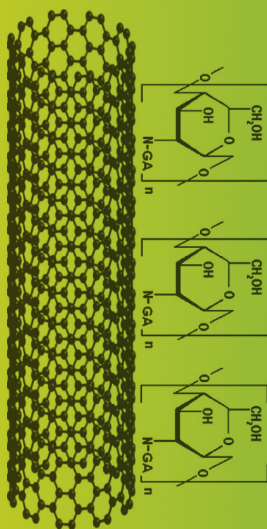
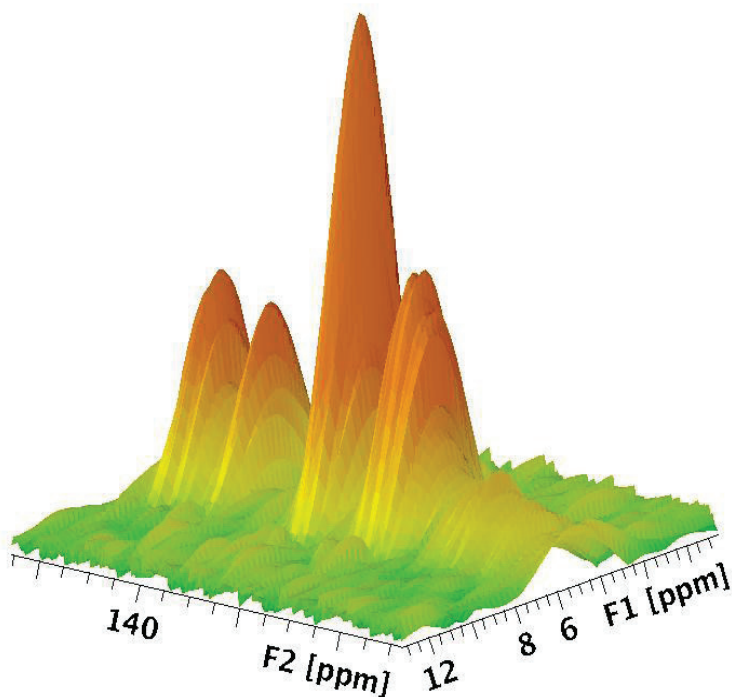


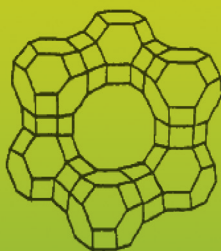
# Solid-State NMR in **MATERIALS SCIENCE**

**Principles and Applications**

Vladimir I. Bakhmutov



**CRC Press**  
Taylor & Francis Group





# **Solid-State NMR in MATERIALS SCIENCE**

**Principles and Applications**



# **Solid-State NMR in MATERIALS SCIENCE**

## **Principles and Applications**

**Vladimir I. Bakhmutov**



**CRC Press**

Taylor & Francis Group

Boca Raton London New York

---

CRC Press is an imprint of the  
Taylor & Francis Group, an **informa** business

CRC Press  
Taylor & Francis Group  
6000 Broken Sound Parkway NW, Suite 300  
Boca Raton, FL 33487-2742

© 2012 by Taylor & Francis Group, LLC  
CRC Press is an imprint of Taylor & Francis Group, an Informa business

No claim to original U.S. Government works  
Version Date: 20110803

International Standard Book Number-13: 978-1-4398-6964-2 (eBook - PDF)

This book contains information obtained from authentic and highly regarded sources. Reasonable efforts have been made to publish reliable data and information, but the author and publisher cannot assume responsibility for the validity of all materials or the consequences of their use. The authors and publishers have attempted to trace the copyright holders of all material reproduced in this publication and apologize to copyright holders if permission to publish in this form has not been obtained. If any copyright material has not been acknowledged please write and let us know so we may rectify in any future reprint.

Except as permitted under U.S. Copyright Law, no part of this book may be reprinted, reproduced, transmitted, or utilized in any form by any electronic, mechanical, or other means, now known or hereafter invented, including photocopying, microfilming, and recording, or in any information storage or retrieval system, without written permission from the publishers.

For permission to photocopy or use material electronically from this work, please access [www.copyright.com](http://www.copyright.com) (<http://www.copyright.com/>) or contact the Copyright Clearance Center, Inc. (CCC), 222 Rosewood Drive, Danvers, MA 01923, 978-750-8400. CCC is a not-for-profit organization that provides licenses and registration for a variety of users. For organizations that have been granted a photocopy license by the CCC, a separate system of payment has been arranged.

**Trademark Notice:** Product or corporate names may be trademarks or registered trademarks, and are used only for identification and explanation without intent to infringe.

**Visit the Taylor & Francis Web site at**  
**<http://www.taylorandfrancis.com>**

**and the CRC Press Web site at**  
**<http://www.crcpress.com>**

---

# Contents

Preface.....	xi
Author .....	xv

<b>Chapter 1</b>	General Principles of Pulsed NMR and NMR Techniques .....	1
1.1	Early History of NMR in the Solid State .....	2
1.2	Nuclei in the External Magnetic Field.....	3
1.3	Effects of Radio Frequency Pulses.....	9
1.4	From Macroscopic Magnetization to Nuclear Relaxation and Shapes of NMR Signals.....	12
1.4.1	Common Representations of Molecular Motions and Their Influence on NMR .....	14
1.4.2	Contribution of Molecular Mobility to Spin–Spin and Spin–Lattice Nuclear Relaxation.....	17
1.5	Parameters Characterizing Nuclei in the External Magnetic Field.....	20
1.5.1	Chemical Shift.....	20
1.5.2	Spin–Spin Coupling .....	22
1.5.3	Quadrupolar Coupling .....	24
1.6	Introducing NMR Equipment and NMR Experiments.....	26
1.6.1	Magnets and NMR Probes .....	28
1.6.2	Homogeneity of the External Magnetic Field and Digital Resolution in NMR Spectra .....	30
1.6.3	Dead Time of NMR Spectrometers: Intensity of Signals and Distortion of Baselines in NMR Spectra .....	30
1.7	Main Principles of Two-Dimensional NMR .....	32
1.8	Enhancement of Sensitivity in NMR .....	34
	References .....	35

<b>Chapter 2</b>	On Amorphous Materials as Potential Objects in Solid-State NMR Studies: Common and Key Problems .....	37
2.1	Hybrid Materials.....	38
2.2	Polymer Solids.....	40
2.3	Systems Based on Nanostructures.....	41
2.4	Wood and Wood Components .....	42
2.5	Glasses .....	44
2.6	Zeolites .....	45

2.7	Design of Porous and Layered Molecular Systems .....	47
2.7.1	General Problems in Structural Characterizations of Amorphous Porous Materials .....	48
2.7.2	Some Key Structural Issues in Characterizations of Amorphous Materials Modified by Metal Ions and Methods for Structure Solution .....	50
	References .....	54
<b>Chapter 3</b>	<b>Features of Solid-State NMR: Diamagnetic Materials .....</b>	<b>57</b>
3.1	From Isotropic Chemical Shifts to Magnetic Shielding Tensors .....	57
3.1.1	Visualization of Chemical Shift Tensors and Determination of Their Orientations.....	62
3.2	Nuclei with a Spin of 1/2 .....	66
3.3	Quadrupolar Nuclei in Solids .....	70
3.3.1	Two Categories of Quadrupolar Nuclei.....	72
3.4	Detection of NMR Signals in Solids: Common Aspects .....	73
3.4.1	Wide-Line NMR .....	73
3.4.2	Direct Excitation .....	74
3.4.3	Cross-Polarization .....	76
3.4.4	Cross-Polarization with Quadrupolar Nuclei .....	79
3.5	High-Power Decoupling .....	81
3.6	Multi-Quantum NMR Experiments .....	83
3.7	Dipolar Recoupling NMR Techniques .....	85
3.8	Sideband Manipulations .....	90
3.9	Zero-Field Solid-State NMR Experiments.....	92
3.10	Solid-State NMR Imaging.....	94
	References .....	96
<b>Chapter 4</b>	<b>Practice of Multinuclear NMR in Diamagnetic Solids: General Information and Examples of Applications .....</b>	<b>99</b>
4.1	Structural Information by Increasing the Spectral Resolution in Multinuclear Solid-State NMR .....	99
4.1.1	Spectral Resolution for Nonquadrupolar Nuclei .....	100
4.1.2	Signal Assignments .....	102
4.1.3	Resolving Quadrupolar Nuclei.....	104
4.2	Probing Proximities of Nuclei and Measurements of Internuclear Distances in Diamagnetic Solids .....	106
4.3	<sup>31</sup> P Solid-State NMR .....	111
4.4	Solid-State NMR of Halogen Nuclei and Oxygen.....	116
4.5	Solid-State NMR of Oxide Materials: Nuclei <sup>51</sup> V, <sup>93</sup> Nb, and <sup>181</sup> Ta.....	123
4.6	Solid-State <sup>13</sup> C NMR: Wood and Wood Products.....	127
4.7	<sup>2</sup> H NMR in Solids at Deuterium Natural Abundance.....	129



4.8	Between Solution- and Solid-State NMR: Nanoparticles and Suspensions.....	131
	References .....	137
<b>Chapter 5</b>	<b>Dynamics in Diamagnetic Materials from Solid-State NMR: Methods, Measurements, and Analysis.....</b>	<b>139</b>
5.1	Variable-Temperature Solid-State NMR Experiments and a Line-Shape Analysis.....	141
5.1.1	Dynamics in Polymeric Materials from a Line-Shape Analysis.....	143
5.2	Molecular Mobility from the Solid-State NMR Relaxation ....	145
5.2.1	Measurements of Relaxation Times and Errors of the Measurements .....	145
5.2.2	How Molecular Motions Affect Nuclear Relaxation ....	149
5.2.2.1	Correlation Time Distribution versus Single Correlation Time .....	151
5.2.3	Relaxation Approaches: Methodology and Examples .....	153
5.3	One- and Two-Dimensional Exchange Solid-State NMR Spectroscopy .....	156
5.4	Molecular Mobility from the Cross-Polarization NMR Experiments .....	158
5.5	Molecular Mobility from Magnetic Relaxation Dispersion Experiments .....	160
	References .....	163
<b>Chapter 6</b>	<b>Strategies in Solid-State Multinuclear NMR: Studies of Diamagnetic Porous Materials.....</b>	<b>165</b>
6.1	Porosity of Materials from NMR .....	165
6.1.1	NMR Cryoporometry.....	168
6.1.2	NMR Relaxometry .....	171
6.1.3	NMR Behavior of Gases in Pore Spaces.....	173
6.2	Structural Features of Silica Lattice and Surface by Solid-State $^1\text{H}$ $^{29}\text{Si}$ , $^{27}\text{Al}$ , and $^{17}\text{O}$ NMR Spectra.....	176
6.2.1	Distribution of Diamagnetic Metal Ions from Solid-State NMR .....	181
6.3	Molecular Mobility in Diamagnetic Porous Materials.....	186
	References .....	189
<b>Chapter 7</b>	<b>Paramagnetic Effects in Solid-State NMR .....</b>	<b>191</b>
7.1	Theoretical Aspects.....	193
7.1.1	Chemical Shifts and Magnetic Shielding Tensors in the Presence of Unpaired Electrons.....	193

7.2	Nuclear Relaxation in the Presence of Unpaired Electrons....	197
7.2.1	Spin Diffusion .....	198
7.2.2	Nuclear Relaxation via Nucleus–Electron Dipolar and Contact Interactions .....	199
7.3	Practical Consequences from the Theory of Paramagnetic Effects .....	200
7.4	$^1\text{H}$ , $^{31}\text{P}$ , $^{13}\text{C}$ , $^2\text{H}$ , $^{29}\text{Si}$ , $^7\text{Li}$ , and $^6\text{Li}$ NMR Spectra of Paramagnetic Solids.....	205
7.5	$^{51}\text{V}$ and $^{55}\text{Mn}$ NMR Spectra of Paramagnetic Solids .....	210
7.5.1	Analyzing the Nature of Metal Ions by Their Direct Observation in Solid-State NMR Spectra.....	212
7.6	Special NMR Techniques for Observations of “Invisible” Target Nuclei.....	215
7.7	Relaxation Measurements and Relaxation Times in Paramagnetic Solids.....	217
7.7.1	Solid-State $T_1$ Measurements .....	224
7.7.2	Spin–Spin Relaxation Times and Anomalies in Solid-State $T_2$ Measurements.....	225
	References .....	228

<b>Chapter 8</b>	Strategy in NMR Studies of Amorphous Porous Paramagnetic Materials.....	231
8.1	Intense Sideband Patterns in MAS NMR Spectra of Paramagnetic Amorphous Materials and Their Analysis .....	231
8.2	Direct Detection of the Nuclei Closest to Paramagnetic Ions in Porous Materials by the Hahn-Echo Mapping NMR Experiments .....	236
8.3	NMR Relaxation Approaches to Structure of Porous Amorphous Paramagnetic Silica-Based Materials: From Experiments to Models and Interpretations.....	240
8.3.1	Factors Affecting Relaxation Times in Porous Solids ...	241
8.3.2	Spin–Lattice Relaxation Times in Porous Silica-Based Materials and Concentrations of Paramagnetic Ions.....	242
8.3.3	$^{29}\text{Si}$ Spin–Lattice and Spin–Spin Relaxation in Static and Spinning Porous Amorphous Paramagnetic Silica-Based Materials .....	243
8.3.4	$T_1$ Criteria for Locations of Paramagnetic Ions: Relaxation of Isotropic Resonances .....	247
8.3.5	$T_1$ Criteria Based on Relaxation of Sideband Patterns in MAS Spectra of Porous Paramagnetic Materials.....	251
8.3.6	BMS Effects and NMR Relaxation of Sideband Patterns in MAS Spectra of Porous Paramagnetic Materials.....	254

8.4	Protocol for Quantification of “Invisible Nuclei” in MAS NMR .....	255
8.5	Concluding Remarks .....	256
	References .....	257



---

# Preface

Nuclear magnetic resonance (NMR), discovered as a physical phenomenon by Bloch and Purcell in 1945, has rapidly become the theoretical basis for a powerful analytical method that is widely applied in different fields of modern fundamental and applied science as well as in medicine and industry. This is easily explained not only by the capability of NMR to solve a large number of practical tasks rapidly, which can be connected with structural descriptions of systems at the macro and/or molecular levels, but also by its capability to identify various types of dynamic behavior often responsible for the mechanical properties of materials.

The development of NMR techniques for solution and solid-state studies is impressive. The areas of NMR applications are constantly expanding from atomic and low-temperature physics (where they are used to monitor multiphoton transitions and probing distortions of magnetic fields in superfluids, respectively) to geology (where they are used to search the pathways of cation diffusion) to archeology (where natural destruction of wood is the focus of investigators).

It is impossible to overestimate the role of NMR in fundamental and applied chemistry where the objects of study are molecular systems varying from simple organic or inorganic compounds to complex biomolecules, such as proteins, and NMR data are collected by one-, two-, and three-dimensional experiments performed on different nuclei.

In 1995, the NMR community celebrated the 50th anniversary of the discovery of NMR in condensed phase emphasizing the strong impact of NMR on the development of different fields of science. While the first NMR experiments were carried out in the gaseous phase by Rabi and coworkers in 1937 to confirm experimentally the ideas of quantum mechanics, at the present time, NMR is an indispensable tool for chemists, biochemists, and biologists. It can be added that different aspects of NMR applications in solutions, liquids, and solids can now be found in the *Encyclopedia of Nuclear Magnetic Resonance* and/or in the *Encyclopedia of Applied Spectroscopy*, which is a remarkable feat by itself for the NMR community.

Generally, chemists apply regular NMR spectroscopy in solutions and/or liquids to characterize, for example, new or currently synthesized compounds and to control chemical reactions. However, even in this context, chemical manipulations can lead to systems that are insoluble in conventional solvents. On the other hand, the principal interests of chemists can be concentrated on the properties and structure of solid molecular systems and composites, which are the focus of materials science. Since the nature, properties, and complexity of new materials change constantly from crystalline to amorphous systems (or systems containing both the phases) and from diamagnetic to paramagnetic materials, solid-state NMR techniques and methodical approaches also change from single-pulse NMR at magic angle spinning (MAS) to various polarization transfers, multiquantum manipulations, and nuclear relaxation measurements performed in static and spinning samples. In fact, according to Dybowski, the literature on solid-state NMR increased by more than 3300

original articles as recently as 2005–2009. This ocean of NMR literature is too large to be studied by chemists, particularly young researchers or beginners in materials science.

Moreover, while in the past NMR spectroscopy and relaxation experiments performed to collect frequency-dependent and time-dependent data, respectively, were two separate areas of research; at the present time, both the domains are equally important for chemists working with complex materials and composites. This is particularly so in the controlled design of new layered and/or porous molecular systems with three-dimensional porous networks, which constitute the most exciting direction of modern materials science. This field needs constant usage of methods capable of a structural analysis of *amorphous heterogeneous* solids and their dynamics. Solid-state NMR and NMR relaxation are ideal tools for solving such tasks; however, they require in-depth knowledge of both techniques. Therefore, this book can serve as a useful reference for researchers as it describes the strategy of solid-state NMR experiments, including theoretical and experimental details, and also considers important technical problems.

This book has been written for the reader who is not familiar with the applications of solid-state NMR. Therefore, it begins by covering the general physical principles of pulsed NMR, by including elements of the theory and practice in the registration of NMR signals, and by explaining different NMR equipment (Chapter 1). This chapter describes the main spectral characteristics, such as chemical shift and spin–spin and quadrupole coupling, and considers NMR sensitivity and its enhancement, including principles of two-dimensional NMR. Chapter 2 introduces some important classes of materials that are potential objects for NMR studies. It formulates key problems of structure and dynamics of these materials and demonstrates the different physical methods used for their resolution.

Chapter 3 describes the important features of solid-state NMR data collected in diamagnetic systems, from isotropic chemical shifts to three-dimensional magnetic shielding in NMR spectra, from nuclei with spins of half to quadrupolar nuclei, often creating problems in their registration. The elements of detection by cross-polarization and multiquantum experiments are also considered. The chapter concludes with a description of sideband manipulations in MAS NMR experiments and briefly touches upon zero-field experiments.

Chapter 4 considers the practice of solid-state NMR applied to diamagnetic systems. It focuses on different practical important questions, from increasing the spectral resolution to principles in the measurement of internuclear distances in solids. General data on solid-state NMR of  $^2\text{H}$ ,  $^{31}\text{P}$ ,  $^{35,37}\text{Cl}$ ,  $^{79/81}\text{Br}$ ,  $^{127}\text{I}$ ,  $^{17}\text{O}$ ,  $^{51}\text{V}$ ,  $^{93}\text{Nb}$ , and  $^{181}\text{Ta}$  nuclei needed for materials scientists are also provided. The chapter concludes by considering the NMR of nanoparticles and suspensions.

Dynamic solid-state NMR is presented in Chapter 5. The chapter introduces the relaxation theory and relaxation time measurements as well as the principles of a line-shape analysis and an exchange NMR spectroscopy for probing molecular mobility in diamagnetic materials.

Chapter 6 describes the strategy of solid-state experiments in different nuclei performed on amorphous porous diamagnetic materials and covers specific NMR approaches to studying distributions of diamagnetic metal ions through silica-based

systems, illustrated by typical examples. NMR porosity experiments are also presented in this chapter.

Chapter 7 is devoted to the theory of paramagnetic effects in solid-state NMR, taking into account chemical shifts and magnetic shielding tensors in the presence of unpaired electrons as a function of nuclear nature. The chapter introduces the theory of nuclear relaxation in the presence of paramagnetic centers in solids, demonstrating the concept of spin–diffusion and electron–nucleus interactions and formulating their relative effectiveness. The theoretical and practical aspects of NMR in metals, specifically, are presented in this chapter.

As a consequence of the theory of paramagnetic effects, Chapter 7 discusses the  $^1\text{H}$ ,  $^{31}\text{P}$ ,  $^{13}\text{C}$ ,  $^{27}\text{Al}$ ,  $^{29}\text{Si}$ , and  $^6\text{Li}$  NMR data collected for static and spinning paramagnetic molecular systems. It demonstrates the specific NMR technique developed for the spectral observation of “invisible” nuclei, which are located close to the paramagnetic centers. Attempts to directly observe the nuclei in paramagnetic centers are also considered. The chapter concludes with  $T_1$ ,  $T_2$  relaxation time measurements and presents some anomalies in the nuclear relaxation behavior of paramagnetic systems.

Chapter 8 discusses the strategy of solid-state NMR experiments performed in different nuclei for some amorphous silica-based paramagnetic materials. These systems are used as examples, revealing possible applications for other complex materials. This chapter provides an analysis of intense sideband patterns typically observed in MAS NMR spectra of paramagnetic systems, discusses the factors affecting relaxation times, and describes the Hahn echo mapping experiments for direct observation of target nuclei in such materials. Finally, it formulates solid-state NMR spectral and relaxation criteria for localization of paramagnetic metal ions in the matrix of materials.

This book has been written in simple language and consists of clear illustrations, numerous examples, and detailed bibliographies. We hope that it will be useful not only for young and experienced researchers in materials science, but also for university and college students.





---

# Author

**Professor Vladimir I. Bakhmutov** has worked in different fields of chemical physics and is the author of more than 300 scientific publications, including topic reviews and books. Among them, two of his books, *Practical Nuclear Magnetic Resonance Relaxation for Chemists* (Wiley & Sons, New York, 2005) and *Ejemplos prácticos del uso de la RMN en la Química* (CINVESTAV, Mexico, 2006), could be of interest to NMR users.



---

# 1 General Principles of Pulsed NMR and NMR Techniques

As has been emphasized in the literature, NMR is capable of performing various tasks rapidly for different objects from homogeneous systems, gases, solutions, and liquids to heterogeneous and strongly amorphous solids. Hence, it is widely used in molecular physics, chemistry, biochemistry, biology, pharmacy, geophysics, materials science, and archaeology. Moreover, nowadays, NMR is the diagnostic method used in veterinary science and medicine particularly in clinical research of the human brain by magnetic resonance imaging (MRI) [1].

A large variety of techniques are applied in NMR spectrometry and MRI. Further, technology is constantly being evolved for studying increasingly complex objects. In other words, new scientific fields demand new NMR techniques, the development of which, in turn, affects these fields. For example, in the past, quick successes in radio frequency technology resulted in the appearance of the first commercial NMR spectrometers in 1953, which strongly impacted research in chemistry, biochemistry, and biology. Then, the synthesis and study of more complex molecular systems, such as biochemical molecular objects and/or complex molecular aggregates, required more powerful NMR spectrometers, with better spectral resolution and sensitivity, modifications in magnet technology for creation of stronger magnetic fields, and development of predominantly new methodological spectroscopic approaches. Thus, the modern commercial NMR spectrometers represent multiple-pulse devices, capable of experiments in solutions and the solid state. They can operate at very high magnetic fields up to 21.14 T and detect even the so-called rare nuclei. In addition, the development of computer techniques and increasing speed of computers, performing very fast Fourier transformation (FT), have led to routine use of the one- (1D), two- (2D), or three-dimensional (3D) NMR applied widely in solutions and the solid state.

This book is devoted to solid-state NMR. In spite of the appearance of the first commercial NMR spectrometers as early as the 1950s, solid-state NMR was not very popular among chemists due to relatively low spectral resolution of the spectrometers and their low sensitivity, which is quite critical for solids. Only in the 1980s did the expansion of solid-state NMR techniques become very rapid.

## 1.1 EARLY HISTORY OF NMR IN THE SOLID STATE

The history of NMR, very interesting and sometimes dramatic, has been reviewed by Andrew and Szczesniak [2]. They note that the first NMR experiments were successfully performed in gases (1937) to experimentally verify theoretical concepts in quantum mechanics by accurately measuring nuclear magnetic moments. However, an attempt by Gorter in 1936 to observe an NMR signal in the condensed phase (that could lead to a new analytical method) was unsuccessful. Gorter attempted to detect resonances of Li nuclei in crystalline LiF and protons in crystalline potassium alum. The second attempt was reported by the same research group 6 years later, where similar experiments were performed for  $^{19}\text{F}$  nuclei in crystal solid KF. Again no signal was observed due to a singularly long relaxation time of  $^{19}\text{F}$  nuclei in these very pure crystals. The important conclusion was that a long relaxation time can cause a saturation effect and resonance lines can become “invisible.” In other words, behavior of target nuclei in NMR experiments is time dependent and expressed as infinitely long relaxation times, particularly in rigid solids free from paramagnetic impurities, and NMR signals are not detected. This important relationship between relaxation times and results observed in NMR experiments is better recognized by theoretical considerations of the relaxation phenomena in Chapter 5.

The first successful observation of NMR signals in the condensed phase was reported by Purcell and Bloch on probing protons in paraffin wax and water, due to their relatively short relaxation times. Finally, Bloembergen, Purcell, and Pound carried out careful investigations of nuclear relaxation and formulated the theory, now known as the BPP theory, which is valid for all states of matter: solids, liquids, and gases. The authors introduced the dipole–dipole mechanism explaining nuclear relaxation via molecular motions characterized quantitatively by correlation times, depending on the nature of objects. It is interesting that after this classic work, other treatments of relaxation processes led to only small changes in the relaxation theory.

One of the first solid objects was ice, showing the principal difference between NMR in solids and liquids: line-width of the  $^1\text{H}$  resonance in liquid water is very small (significantly  $<1$  Hz) while the resonance of ice is dramatically broadened up to  $\sim 10^5$  Hz. This effect related to strong magnetic dipolar proton–proton interactions is the second factor that complicates observation of NMR signals in solids. It became obvious that detection of NMR signals in liquid water and ice requires different technical solutions.

It is significant that the first simple, noncommercial NMR spectrometer was created in 1946, capable of resonance observations in liquids and solids as well as measurement of relaxation times necessary for detailed understanding of the role of molecular motions in the NMR phenomenon. In 1947 extremely low temperature relaxation measurements were performed in solid  $\text{H}_2$  at a temperature of 1 K to reconfirm the importance of molecular motions in the dipole–dipole relaxation process. In spite of these successes, the relaxation mechanism operating in such crystals as  $\text{CaF}_2$  remained unclear. Only in 1949 did Bloembergen explore the nature of this mechanism via energy diffusion from nuclear spins to centers containing unpaired electrons, due to their dipolar coupling [3]. The cycle of these classic works was especially important because it became clear that the NMR spectrum in solids,

namely, widths of the resonances and their shapes, are dictated by magnetic dipolar nuclear interactions, while relaxation of nuclei occurs due to a time dependence of these interactions.

In the context of practical applications of NMR, important for chemists, the aforementioned statement can be reformulated as the NMR spectra in solids contain information about the number of nuclei in structurally different molecules and/or groups and their mutual dispositions, while nuclear relaxation time measurements at different temperatures open the way to understanding the dynamic behavior of these groups and molecules from isotropic and anisotropic reorientations to phase transitions. These two unique features allow us to consider solid-state NMR as a powerful analytical method, including NMR techniques based on magic angle spinning, multiple pulse sequences, cross-polarization, double and triple resonance, nuclear Overhauser effect (NOE), and experiments in zero fields [2], which are considered in this book.

## 1.2 NUCLEI IN THE EXTERNAL MAGNETIC FIELD

Generally the structural chemistry of materials requires determination of the number of molecules in structural units and their symmetry in the lattice of materials. Solid-state NMR gives a solution for this general task. Moreover some NMR approaches, as an alternative of the x-ray diffraction method, can even provide accurate internuclear distances or bond angles, for example, angles Si–O–Si in glasses that are determined on the basis of relationships between the line dispositions in the NMR spectra and the structural parameters. All these points are directly related to definitions of chemical shifts, line shapes, line widths, and spectral resolution, as fundamental properties of nuclear behavior in the external magnetic field.

In spite of the great variety of NMR experiments and NMR techniques [4–8], the physical meaning of NMR can be reformulated in a simple form as follows: *nuclei are placed into the external magnetic field and excited by a radio frequency irradiation; then, the resulting absorbed energy is registered as NMR signals*. These signals form the NMR spectra recorded usually as plots in the axes “line intensity/resonance frequency.”

Dispositions of resonance lines in the NMR spectra are characterized by chemical shifts generally measured in ppm (Figure 1.1). The fine splitting of the NMR signals due to quadrupole coupling or spin–spin coupling (Figure 1.2) is measured in Hz and depends on electronic environments of nuclei. Finally, integral intensities of the signals are proportional to the number of the nuclei, when the nuclei are excited directly and relaxed completely. That is why the NMR spectra are directly related to molecular structures.

It should be emphasized that the spin–spin coupling constants regularly used by chemists to elucidate molecular structures in solution are also important for the solid-state NMR spectra. It is obvious, however, that they should be well resolved (e.g., the *high resolution* can be reached in magic angle spinning [MAS] NMR spectra). Figure 1.1 shows clearly the presence of spin–spin coupling constant  $^1J(^{13}\text{C}-^{199}\text{Hg})$  in the  $^{13}\text{C}\{^1\text{H}\}$  CP MAS NMR spectrum of the mercury complex in Scheme 1.1. This complex forms in the solid state a network typical of porous materials capable of gas absorption [9]. As the scheme shows, the  $^{13}\text{C}$  resonance appearing at  $\sim 160$  ppm

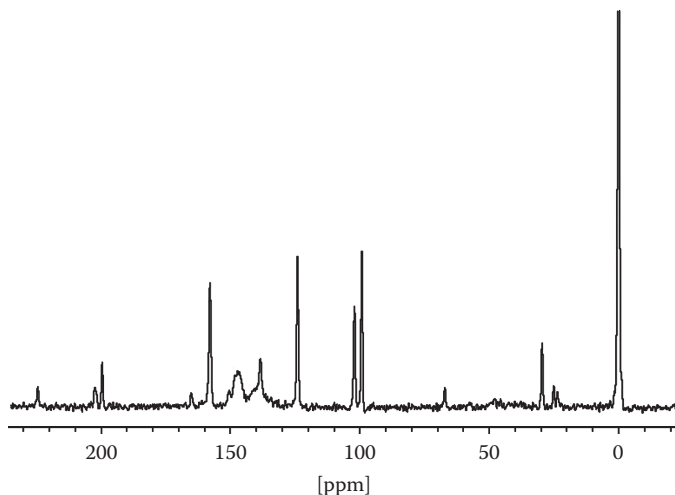


**FIGURE 1.1** The solid-state  $^{13}\text{C}$  CP MAS NMR spectrum of a porous material created by a network of the compounds in Scheme 1.1. The spectrum was recorded at a spinning rate of 10 kHz with a standard 4 mm NMR rotor. The mixing time for cross-polarization was 1500  $\mu\text{s}$  at a  $90^\circ$  ( $^1\text{H}$ ) pulse of 4  $\mu\text{s}$ .  $^1\text{H}$  Decoupling was provided by a tppm-pulse sequence operating at  $^1\text{H}$  frequency. The relaxation delay was 5 s.

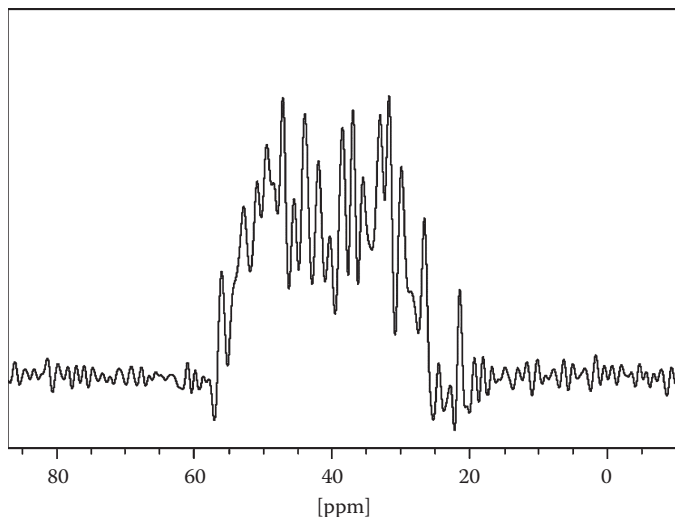
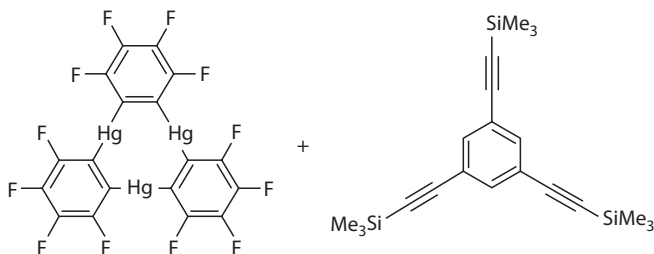


**FIGURE 1.2** The solid-state single-pulse  $^{19}\text{F}$  MAS NMR spectrum of compound  $\text{Fe(II)}_5(\text{bptz})_4(\text{SbF}_6)_{10}(\text{CH}_3\text{CN})_{10}$ , recorded at a spinning rate of 12 kHz with a standard 4 mm NMR rotor, a  $60^\circ$ -( $^{19}\text{F}$ ) pulse and relaxation delay of 6 s. The high-resolution spectrum was obtained due to the Gauss treatment provided by standard software to increase the spectral resolution. Therefore, the initial NMR data were collected with a relatively large memory size of 16k and at a large number of scans to reach a good signal-to-noise ratio.



**SCHEME 1.1** The molecular system based on the mercury complex forming in the solid state a network typical of porous materials capable of gas absorption.

is accompanied by two satellites separated by 1483 Hz. First, observations of the  $J$  constants simplify spectral assignments that play a major role in structural analysis. Second, for example, accurate measurements of these  $^1J(^{13}\text{C}-^{199}\text{Hg})$  magnitudes can potentially show the changing electronic density on carbon and mercury atoms in chemical modifying systems of this family.

The second intriguing example is represented in Figure 1.2, where the  $^{19}\text{F}$  MAS NMR spectrum of solid compound  $\text{Fe}(\text{II})_5(\text{bptz})_4(\text{SbF}_6)_{10}(\text{CH}_3\text{CN})_{10}$  reported by Campos-Fernández et al. [10] exhibits a  $^{19}\text{F}$  resonance consisting of 20 lines, at least. A portion of the lines corresponds to the  $^1J(^{19}\text{F}-^{121}\text{Sb})$  constant of 1940–1950 Hz, while the second part shows the  $^1J(^{19}\text{F}-^{123}\text{Sb})$  splitting of 1033 Hz. Since the isotopic shift ( $^{19}\text{F}-^{121,123}\text{Sb}$ ) is not detectable in the solid state due to relatively low spectral resolution, the number of the observed lines proves the presence of three nonequivalent ions  $[\text{SbF}_6]^-$  in this solid compound, one of which can be encapsulated in the bptz cycle in accordance with a single crystal x-ray structure. In addition, the absence of a  $J(^{19}\text{F}-^{19}\text{F})$  splitting demonstrates equivalency of  $^{19}\text{F}$  nuclei. This equivalency, in turn, proves fast isotropic reorientations of  $[\text{SbF}_6]^-$  ions.

The practical importance of chemical shift and spin–spin coupling is obvious from the earlier examples. Both of them originate from the behavior of nuclei placed into the external magnetic field. This behavior is generally described in terms of nuclear spins, represented via wave functions,  $\psi$ , similar to electron wave functions. These  $\psi$  functions depend on the spatial and spin coordinates and can be used to calculate energy of spin states via Schrödinger's equation,  $\hat{H}\psi = E\psi$ , where  $\hat{H}$  is an operator (*Hamiltonian*) that acts on the wave function. Then, spin operator  $\hat{I}$  with components  $\hat{I}_x$ ,  $\hat{I}_y$ , and  $\hat{I}_z$  corresponds to the spin coordinates of the wave functions [11]. This quantum mechanical formalism finally leads to energy levels whose appearance in the external magnetic field explains the phenomenon of NMR. A semiclassical description of the NMR effect is also possible, where a central role belongs to behavior of the net magnetization created in a sample that is placed in the external magnetic field. Both of these approaches are partially used in the following.

According to the aforementioned formalism (see, e.g., Abragam [4]), any nucleus is magnetically active when it possesses a *nonzero angular momentum*,  $P$ . It is significant that most of the elements in the periodic table have magnetically active isotopes with different natural magnetic abundance. The rule is simple: a nucleus has a zero spin when numbers of protons and neutrons are equal.

The angular momentum  $P$  is responsible for appearance of *nuclear magnetic moment*,  $\mu$ , which is expressed via,

$$\mu = \gamma P \quad (1.1)$$

In turn, nuclear momentum  $\mu$  is capable of responding to the presence of the external magnetic field, noted in the following as  $B_0$ . Coefficient  $\gamma$  in Equation 1.1, representing the nuclear magnetogyric ratio is one of the fundamental magnetic nuclear constants dependent on the nuclear nature. Table 1.1 lists some magnetic properties for the nuclei that are most popular as target nuclei for materials chemists. First, as the table shows, the  $\gamma$  values change in a very large diapason illustrating, thus, a very large diapason of resonance frequencies. Second, the  $\gamma$  constant has a sign that plays an important role in some NMR experiments; for example, at indirect detection of nuclei. Finally, it should be emphasized that sensitivity, as a very important parameter in NMR experiments, fundamentally depends on the nuclear nature, that is, on magnetogyric constants of nuclei and their natural abundance. For example, sensitivity related to  $^1\text{H}$  nuclei reduces by factor of  $\sim 10^3$ ,  $10^4$ , and  $10^6$  in going to  $^{117}\text{Sn}$ ,  $^{13}\text{C}$ , and  $^2\text{H}$  nuclei, respectively. This circumstance sometimes creates significant problems in detection of NMR signals, particularly in the solid state where

**TABLE 1.1**  
**NMR Properties of Selected Nuclei**

Nucleus	Spin I	Natural Abundance (%)	NMR Frequency, $\nu_0$ , in MHz at $B_0 = 2.3488 \text{ T}$	$\gamma$ ( $10^7 \text{ rad/Ts}$ )
$^1\text{H}$	1/2	99.98	100	26.752
$^2\text{H}$	1	0.016	15.35	4.107
$^{11}\text{B}$	3/2	80.42	32.08	8.584
$^{13}\text{C}$	1/2	1.108	25.14	6.728
$^{14}\text{N}$	1	99.63	7.22	1.934
$^{15}\text{N}$	-1/2	0.366	10.14	-2.712
$^{29}\text{Si}$	-1/2	4.67	19.87	-5.319
$^{19}\text{F}$	1/2	100	94.08	25.18
$^{31}\text{P}$	1/2	100	40.48	10.84
$^{17}\text{O}$	-5/2	0.037	13.557	-3.628
$^{93}\text{Nb}$	9/2	100	24.549	6.567
$^{51}\text{V}$	7/2	99.75	26.3	7.036
$^{59}\text{Co}$	7/2	100	23.7	6.347
$^{109}\text{Ag}$	-1/2	48.2	4.65	-1.083
$^{117}\text{Sn}$	1/2	7.61	35.63	-9.578
$^{119}\text{Sn}$	1/2	8.58	37.29	-10.02
$^{129}\text{Xe}$	-1/2	26.4	27.8	-7.399
$^{113}\text{Cd}$	-1/2	12.2	22.2	-5.933
$^{199}\text{Hg}$	1/2	16.84	17.91	4.815
$^{205}\text{Tl}$	1/2	70.5	57.63	15.589



resonances can be strongly broadened due to strong dipolar internuclear interactions and relaxation times are elongated.

As follows from Table 1.1,  $^1\text{H}$  and  $^{19}\text{F}$  nuclei are most convenient in chemical investigations by the NMR method due to their natural abundance. On the other hand, these nuclei undergo the strongest dipolar interactions, complicating their detection with high resolution and requiring a special technique for collection of the data.

The  $P$  and  $\mu$  magnitudes are *quantized* and projections of the angular nuclear moment,  $P_z$ , on the OZ coordinate axis shown in Figure 1.3 can be written as follows:

$$P_z = \hbar m_l$$

$$\hbar = \frac{h}{2\pi} \quad (1.2)$$

where

$\hbar$  is Planck's constant ( $h/2\pi = 1.05457266 \times 10^{-34}$  J s)

$m_l$  is the magnetic quantum number dependent on the nuclear spin,  $I$ , taking values from  $I$  to  $-I$  as:  $I, I - 1, I - 2 \dots -I$

In turn, according to the quantum-mechanical formalism,  $I$  is a multiple of  $1/2$ . For example, at  $I = 1/2$  the angular and magnetic moments can be expressed by

$$P_z = \pm \left( \frac{1}{2} \right) \hbar$$

$$\mu_z = \pm \left( \frac{1}{2} \right) \gamma \hbar \quad (1.3)$$

Hence, the  $\mu_z$  (or  $P_z$ ) projections, which are imagined in the following as vectors, take only two "permitted" spatial orientations: *parallel* or *antiparallel* relative to the OZ axis. It should be emphasized that in the absence of the external magnetic field  $B_0$  both of the orientations are obviously energetically equivalent and thus the nuclei occupy a single energy level.

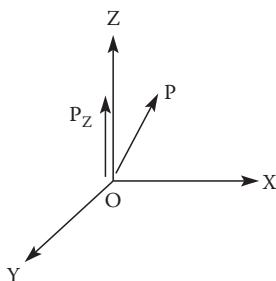


**FIGURE 1.3** Projection of the nuclear angular moment  $P$ ,  $P_z$ , on the OZ axis. The external magnetic field,  $B_0$ , is generally applied along the OZ direction, while the radio frequency field affecting the  $P_z$  projection is applied along the OX (or OY) coordinate.

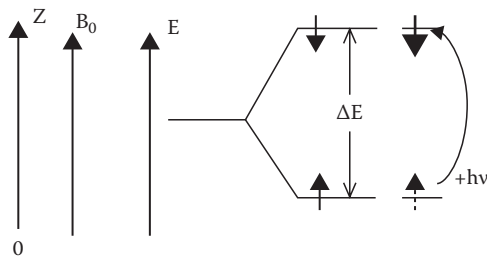


**FIGURE 1.4** Zeeman's energy levels that appear for nuclear spins  $I = 1/2$  placed into the external magnetic field,  $B_0$ , applied along the OZ coordinate.

When the strong magnetic field is applied, for example, along the OZ axis, the aforementioned parallel or antiparallel  $\mu_z$  (or  $P_z$ ) orientations become nonequivalent. Then, the initially degenerated energy level undergoes the so-called Zeeman's splitting shown in Figure 1.4 and this splitting  $\Delta E$  expressed via Hamiltonian (1.4) will be proportional to the  $\mu_z$  magnitude and the strength of the applied magnetic field,  $B_0$ :

$$\hat{H} = \gamma \hbar \hat{I} B_0 \quad \text{and} \quad \Delta E = 2\mu_z B_0 \quad (1.4)$$

Since a minimal energy difference can be formulated as *one quantum*,

$$\Delta E = h\nu \quad (1.5)$$

Equation 1.4 can be rewritten as

$$\begin{aligned} h\nu_0 &= 2\mu_z B_0 = \gamma \hbar B_0 \\ \nu_0 &= \gamma B_0 \end{aligned} \quad (1.6)$$

formulating, thus, the fundamental conditions of the resonance phenomenon for a single uncoupled nucleus: the nucleus, characterized by the  $\gamma$  constant and the spin of  $1/2$ , is placed into the external magnetic field,  $B_0$ , and undergoes a single-quantum transition (i.e., the  $m_I$  number changes from  $-1/2$  to  $+1/2$ ) between the Zeeman's energy levels from a low energy to a high energy level at radio frequency irradiation with frequency  $\nu_0$ . Following from the equations, the  $\nu_0$  frequency, named Larmor's frequency, depends on the nature of the nuclei and the strength of the applied magnetic field,  $B_0$ .

For nuclei with spin  $\geq 1$ , named quadrupolar nuclei, the number of energy levels obviously increases. For example,  $^2\text{H}$  or  $^{14}\text{N}$  nuclei with spin  $I = 1$ , produce three energy levels, corresponding to the  $\mu_z$  values of  $+\gamma\hbar(1)$ ,  $0$  and  $-\gamma\hbar(1)$ . It should be noted that in solutions and liquids this circumstance does not complicate the situation because, on the one hand, the levels are energetically equidistant, and on the other hand the double quantum nuclear transitions (the  $m_I$  value changes from  $+1$  to  $-1$ ) are forbidden. For this reason, in spite of the presence of three energy levels in solutions, the nuclear transitions between them are registered as a single NMR resonance.

In contrast, a larger number of the energy levels for quadrupolar nuclei strongly affect the shape of NMR signals in the solid state. Here besides the strongly intense transitions from  $-1/2$  to  $+1/2$ , other transitions can be also excited and detected. As is seen in the following, such an excitation can lead to very wide sideband patterns in the MAS NMR spectra of quadrupolar nuclei.

### 1.3 EFFECTS OF RADIO FREQUENCY PULSES

As the previous section shows, an NMR signal can be detected when the frequency of irradiation approaches the Larmor frequency  $\nu_0$  due to absorption of energy  $\Delta E$ . Technically the continuous wave (CW) irradiation methods have been used in the earliest NMR experiments to observe *change in macroscopic magnetization* that is created in a sample in the presence of the  $B_0$ . In these terms, the sample is considered as an ensemble of nuclei that populate the Zeeman's energy levels proportionally to the factor

$$\exp\left(-\frac{\Delta E}{kT}\right) \quad (1.7)$$

where

T is the temperature

k is Boltzmann's constant (measured as  $1.380658 \times 10^{-23}$  J/K)

Under these conditions, the unequal populations of the energy levels in the external magnetic field produce the equilibrium macroscopic magnetization that undergoes Larmor's precession, as shown in Figure 1.5. The frequency of this precession is  $\nu_0$  or  $\omega_0 = 2\pi\nu_0$  and the CW  $\nu_0$  irradiation reorients the magnetization vector that is directly registered as an NMR spectrum.

Besides the CW irradiation the resonance can be reached with the help of radio frequency pulses (RFPs). By definition, a powerful radio frequency (RF) pulse at acting frequency  $\omega_{rf}$  can simultaneously excite a very large frequency band resulting

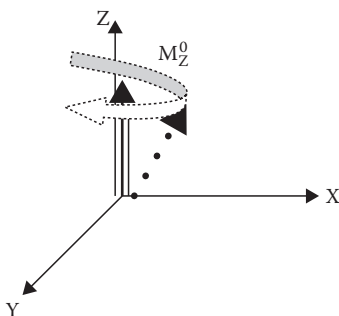


**FIGURE 1.5** The macroscopic magnetization  $M_Z^0$  is created in a sample in the presence of the external magnetic field  $B_0$  oriented along the OZ coordinate. The interaction between the  $M_Z^0$  and the  $B_0$  leads to the Larmor precession with frequency  $\nu_0$  or  $\omega_0 = 2\pi\nu_0$  as an equilibrium state of a nuclear system.

in appearance of a *time-dependent* oscillating field. This field contributes to the external magnetic field  $B_0$  to produce a total field that can be expressed as

$$B_{\text{total}} = iB_1 \cos(\omega_{\text{rf}}t) + kB_0 \quad (1.8)$$

Here, the unit vector  $i$  is situated along the OX direction and the unit vector  $k$  is along the OZ direction. Under these conditions, the Hamiltonian can be transformed to the form

$$\hat{H} = -\gamma\hbar(\hat{I}_Z B_0 + \hat{I}_X B_1 \cos(\omega_{\text{rf}}t)) \quad (1.9)$$

Now, the expression contains the rotating component, and the wave function,  $\psi'$ , describing spin states in the new rotating coordinate system takes a form (1.10)

$$\psi' = \exp(-i\psi_{\text{rf}}t \hat{I}_Z) \times \psi \quad (1.10)$$

where the first term represents the rotation operator. The accurate quantum-mechanical description of the spin system and the corresponding solution of Schrödinger's equation are not simple and they can be found, for example, in the literature [4,5]. The aforementioned equation is just to show that description of spin states under action of a RF pulse requires introduction of the new rotating coordinate system. Broadly, the nuclear behavior can be easily imagined by a vector model shown in Figure 1.6.

Here magnetization vector  $M$ , orientated at an equilibrium state along the OZ direction in a rotating coordinate system, undergoes reorientations by the action of RF pulses at their different durations. It should be emphasized that durations and amplitudes of RF pulses should be sufficient to rotate the magnetization vector, for example, by angle  $\alpha$ . According to the Ernst rule [12], the pulse angle,  $\alpha$ , is defined as

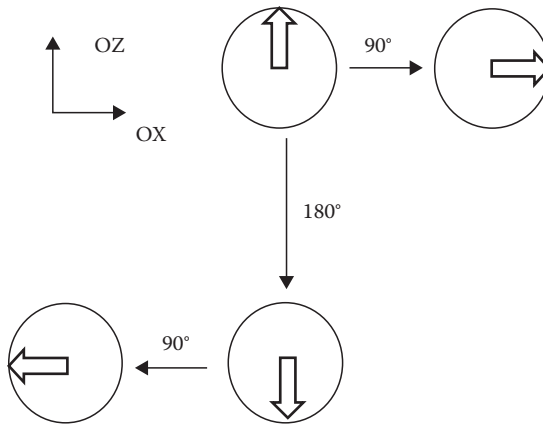


**FIGURE 1.6** A simple vector representation, visualizing how the magnetization vector changes the orientation in the rotating frame by the action of RFP of  $90^\circ$  and  $180^\circ$  or their combination.